



Damage Model for Composites Defined in Terms of Available Data

EVER J. BARBERO

Department of Mechanical and Aerospace Engineering, West Virginia University, Morgantown, West Virginia, USA

PAOLO LONETTI

Universita degli Studi della Calabria, Arcavacata di Rende, Italy

ABSTRACT

A model to predict stiffness reduction and stress redistribution due to damage of laminated polymer composites is presented. The material properties required by the model are limited to those already available for unidirectional composites. Classical lamination theory is generalized for the case of a continuously damaging material using concepts from continuous damage mechanics. The Tsai-Wu failure criteria can be recovered as a limiting case. The damage model is validated with experimental results for various laminates built with aramid/epoxy, T300/5208, and T300/914 carbon/epoxy.

A fiber-reinforced polymer matrix composite is inhomogeneous, but can be modeled as an anisotropic homogeneous material. The elastic stiffness of such homogeneous material can be predicted with great success in terms of the properties of the constituent phases (fiber and matrix) using micromechanics [1]. Since strength properties cannot be accurately predicted, most designers rely on experimental properties. The strength values are measured as ultimate failure values in uniaxial tests. Such failures usually occur after significant internal damage with concomitant reduction in stiffness [2-4]. The evolution of stiffness from the threshold of damage to the failure of the material is important [5-7]. Significant stress redistribution is to be expected among the layers in a laminate and among various loads paths in the structure if the material undergoes damage. Predictions of ultimate load for laminate composites based on ply discount or fudge degradation factors (see Section 7.2.2 in [1]) are usually not reliable [8].

Several types of modeling have been attempted in an effort to predict the behavior of the damaged laminate prior to failure. First, approximate methods such as ply discount and adjustable degradation factors have been used with limited success [8]. Second, micromechanical models have been used to assemble the global response of a single ply in terms of the damaging behavior of the constituents [9-11]. Such models have not been

Received 2 October 2000; accepted 4 April 2001.

The financial support of Ever J. Barbero by the National Science Foundation (USA) through Grant CMS-9612162 and of Paolo Lonetti by the Ministero della Universita a della Ricerca Scientifica (Italy) are gratefully acknowledged.

Address correspondence to Prof. Ever J. Barbero, Construction Facilities Center, Department of Mechanical and Aerospace Engineering, West Virginia University, Morgantown, WV 26506-6101, USA. E-mail: ejbarbero@mail.wvu.edu

extended to deal with laminates because they are computationally intensive, they require a large number of material parameters, and there is no systematic methodology for finding the parameters from experimental data. Third, continuous damage mechanics models rely on a phenomenological description of the damage process and require a smaller number of parameters [2]. However, existing models require special testing techniques or testing of nonstandard laminates to determine the additional material parameters. Such test data are generally not available and not likely to be generated because of the high cost of material testing and the large number of material systems available in the marketplace. Furthermore, no standard tests methods (ASTM and/or ISO) exist for such special tests. On the other hand, standard test methods exist and have been used to evaluate most of the stiffness and strength values for a unidirectional ply of most commercial systems [12]. Therefore, the objective of this article is to present a model for damage of laminated composites based exclusively on available data. To accomplish this objective requires a number of simplifying assumptions such as assuming that the effects of friction are negligible. Although frictional effects at the fiber–matrix interphase and laminae interfaces may be present, they are not considered in this work. This is necessary to avoid the complexity of a nonconvex problem. Although many experimental studies show stiffness degradation during fatigue loading [7], for the sake of simplicity, the proposed model addresses only monotonic loading. Consequently, the model has been validated with monotonic loading only [13–16]. In addition, the present model, being set in the framework of continuum damage mechanics, deals with the homogenized response only. Therefore, the model cannot predict the microscopic features of damage such as crack spacing and periodicity [5–7]. It can only predict the reduction of stiffness and consequent redistribution of stress among laminae. Finally, the model assumes a two-dimensional plane stress field at the meso-scale (lamina) level, neglecting the three-dimensional effects at the crack tip [6]. In summary, all microstructural details are averaged, using continuous damage mechanics concepts, in an attempt to develop the simplest model that still can predict stiffness degradation in an average sense.

§1. CLASSICAL LAMINATION THEORY WITH DAMAGING LAYERS

First, provision is made to model the stress redistribution in the laminate that occurs as a result of the reduction in stiffness due to damage. When a laminate is under bending, the strain distribution is linear through the thickness. Therefore, the material damages nonuniformly through the thickness of the laminate. As a result, the material properties vary continuously but linearly through the thickness of each ply. Therefore, the damage-reduced stiffness matrix in the material directions is defined by a linear function of the material property of the top and bottom of the k th layer. as follows:

$$Q_{i,j}^d(z) = Q_{i,j}^d(z_k^{\text{bot}}) + \frac{Q_{i,j}^d(z_k^{\text{top}}) - Q_{i,j}^d(z_k^{\text{bot}})}{(z_k^{\text{top}} - z_k^{\text{bot}})}(z - z_k^{\text{bot}}) \quad (1)$$

Using the standard coordinate transformation equations [4], the constitutive equations in the global directions for $Z = Z_k$ are

$$\begin{bmatrix} \sigma_x \\ \sigma_y \\ \sigma_{xy} \end{bmatrix}^{Z_k^{\text{top, bottom}}} = \begin{bmatrix} \bar{Q}_{11}^d & \bar{Q}_{12}^d & \bar{Q}_{16}^d \\ \bar{Q}_{12}^d & \bar{Q}_{22}^d & \bar{Q}_{26}^d \\ \bar{Q}_{16}^d & \bar{Q}_{26}^d & \bar{Q}_{66}^d \end{bmatrix}^{Z_k^{\text{top, bottom}}} \begin{bmatrix} \varepsilon_x \\ \varepsilon_y \\ \gamma_{xy} \end{bmatrix}^{Z_k^{\text{top, bottom}}} \quad (2)$$

where the tension σ over the layer is

$$\sigma_i(z) = \sigma_i(Z_k^{\text{bot}}) + \frac{\sigma_i(Z_k^{\text{top}}) - \sigma_i(Z_k^{\text{bot}})}{(Z_k^{\text{top}} - Z_k^{\text{bot}})}(z - Z_k^{\text{bot}}) \quad (3)$$

The laminate stiffness matrix (Eq. 6.15 in [1]) is obtained by integrating the stress resultants (Eq. 6.12 in [1]) but using the damaged, plane stress constitutive Eq. (2), obtaining equations similar to (Eq. 6.16 in [1]) but in terms of damaged values \bar{Q}_{ij}^d , which can be written explicitly as

$$\begin{aligned} D_{i,j} &= \frac{1}{12}(Z_k^{\text{top}})^3 \frac{(3 \cdot \bar{Q}_{i,j}^d(Z_k^{\text{top}}) \cdot Z_k^{\text{top}} + \bar{Q}_{i,j}^d(Z_k^{\text{bot}}) \cdot Z_k^{\text{top}} - 4 \cdot \bar{Q}_{i,j}^d(Z_k^{\text{top}}) \cdot Z_k^{\text{bot}})}{(Z_k^{\text{top}} - Z_k^{\text{bot}})} \\ &+ \frac{1}{12}(Z_k^{\text{bot}})^3 \frac{(\bar{Q}_{i,j}^d(Z_k^{\text{top}}) \cdot Z_k^{\text{bot}} + 3 \cdot \bar{Q}_{i,j}^d(Z_k^{\text{bot}}) \cdot Z_k^{\text{bot}} - 4 \cdot \bar{Q}_{i,j}^d(Z_k^{\text{bot}}) \cdot Z_k^{\text{top}})}{(Z_k^{\text{top}} - Z_k^{\text{bot}})} \\ B_{i,j} &= \frac{1}{6}(Z_k^{\text{top}})^2 \frac{(2 \cdot \bar{Q}_{i,j}^d(Z_k^{\text{top}}) \cdot Z_k^{\text{top}} + \bar{Q}_{i,j}^d(Z_k^{\text{bot}}) \cdot Z_k^{\text{top}} - 3 \cdot \bar{Q}_{i,j}^d(Z_k^{\text{top}}) \cdot Z_k^{\text{bot}})}{(Z_k^{\text{top}} - Z_k^{\text{bot}})} \\ &+ \frac{1}{6}(Z_k^{\text{bot}})^2 \frac{(\bar{Q}_{i,j}^d(Z_k^{\text{top}}) \cdot Z_k^{\text{bot}} + 2 \cdot \bar{Q}_{i,j}^d(Z_k^{\text{bot}}) \cdot Z_k^{\text{bot}} - 3 \cdot \bar{Q}_{i,j}^d(Z_k^{\text{bot}}) \cdot Z_k^{\text{top}})}{(Z_k^{\text{top}} - Z_k^{\text{bot}})} \\ A_{i,j} &= \frac{1}{2}Z_k^{\text{top}} \frac{(\bar{Q}_{i,j}^d(Z_k^{\text{top}}) \cdot Z_k^{\text{top}} + \bar{Q}_{i,j}^d(Z_k^{\text{bot}}) \cdot Z_k^{\text{top}} - 2 \cdot \bar{Q}_{i,j}^d(Z_k^{\text{top}}) \cdot Z_k^{\text{bot}})}{(Z_k^{\text{top}} - Z_k^{\text{bot}})} \\ &+ \frac{1}{2}Z_k^{\text{bot}} \frac{(\bar{Q}_{i,j}^d(Z_k^{\text{top}}) \cdot Z_k^{\text{bot}} + \bar{Q}_{i,j}^d(Z_k^{\text{bot}}) \cdot Z_k^{\text{bot}} - 2 \cdot \bar{Q}_{i,j}^d(Z_k^{\text{bot}}) \cdot Z_k^{\text{top}})}{(Z_k^{\text{top}} - Z_k^{\text{bot}})} \end{aligned} \quad (4)$$

§2. THE DAMAGE MODEL

The damage model is described in this section. It accounts for damage initiation, damage evolution, and failure at the critical values of the damage measures corresponding to each mode of deformation. Using the concepts of continuous damage mechanics [2], the effective stress can be computed in terms of the apparent stress as

$$\bar{\sigma}_{ij} = M_{ijkl}^{-1}(D)\sigma_{kl} \quad (5)$$

where the fourth-order tensor \mathbf{M} is obtained from the second-order integrity tensor as $M_{ijkl} = \Omega_{ik}\Omega_{lj}$. In turn, the integrity tensor Ω is given in term of the damage tensor \mathbf{D} as $\Omega = \sqrt{\mathbf{I} - \mathbf{D}}$, where \mathbf{I} is the second-order identity tensor [17].

In the sequel, the lamina material directions are used as the reference frame. The damage principal directions are assumed to be coincident with the lamina material directions throughout the damage process. Then, the damage tensor \mathbf{D} is characterized by its eigenvalues and can be represented as a three-component array $[D] = [D_1, D_2, D_3]^T$.

Since the damage described by \mathbf{D} and \mathbf{M} is orthotropic, initial undamaged transverse isotropy of the composite can evolve into orthotropy by way of the damaged stiffness tensor, computed as

$$\bar{E} \varphi = M : \bar{E} : M^T \quad (6)$$

Moreover, each fiber-reinforced composite lamina is characterized by a state of plane stress. Although the principal directions of stress do not necessarily coincide with the material coordinate system within a lamina, the principal directions of the damage tensor are assumed to coincide with the material directions, e.g., fiber, transverse, and thickness directions. This is consistent with the view that the dominant modes of damage are either parallel or normal to the fiber direction. Such modes of failure include matrix cracking, fiber matrix debonding, fiber breakage, and delaminations, among others.

In the sequel, contracted notation [1] is used, so that the stress tensor can be represented in the damage principal frame as a three-component array. Using Eq. (5), the effective stress and strain components become

$$\begin{aligned}\bar{\sigma}_1 &= \sigma_1 \Omega_1^{-2} & \bar{\varepsilon}_1 &= \varepsilon_1 \Omega_1^2 \\ \bar{\sigma}_2 &= \sigma_2 \Omega_2^{-2} & \bar{\varepsilon}_2 &= \varepsilon_2 \Omega_1^2 \\ \bar{\sigma}_6 &= \sigma_6 \Omega_1^{-1} \Omega_2^{-1} & \bar{\varepsilon}_6 &= \varepsilon_6 \Omega_1 \Omega_2\end{aligned}\quad (7)$$

Finally, the components of the second-order thermodynamic force tensor \mathbf{Y} , dual to the damage tensor \mathbf{D} , can be derived from strain energy of the damaged material as

$$Y_{ij} = -\frac{1}{2} \frac{\partial (E_{pqrs} \varepsilon_{pq} \varepsilon_{rs})}{\partial D_{ij}} \quad (8)$$

where \mathbf{E} is the damaged stiffness tensor and ε is the second-order damaged-strain tensor. Since the damage model is based on equivalent strain energy between damaged and undamaged configuration, the damaged strain is different from the undamaged one [2]. Using Eqs. (7) and (8) and taking into account the state of plane stress in the lamina, we get

$$\begin{aligned}Y_1 &= \frac{1}{\Omega_1^2} \left(\frac{\bar{C}_{11}}{\Omega_1^4} \sigma_1^2 + \frac{\bar{C}_{12}}{\Omega_1^2 \Omega_2^2} \sigma_1 \sigma_2 + \frac{\bar{C}_{66}}{\Omega_1^2 \Omega_2^2} \sigma_6^2 \right) \\ Y_2 &= \frac{1}{\Omega_2^2} \left(\frac{\bar{C}_{22}}{\Omega_2^4} \sigma_2^2 + \frac{\bar{C}_{12}}{\Omega_1^2 \Omega_2^2} \sigma_1 \sigma_2 + \frac{\bar{C}_{66}}{\Omega_1^2 \Omega_2^2} \sigma_6^2 \right) \\ Y_3 &= 0\end{aligned}\quad (9)$$

where $\bar{C} = \bar{E}^{-1}$ is the fourth-order effective elastic compliance, that is, the compliance of the virgin, undamaged material.

The existence of a damage surface that separates the undamaged state from the damaged one is supported by experimental evidence in the case of fibrous composites. For example, acoustic emissions associated with the nucleation of cracks and defects were used on unidirectional fiber-reinforced composites [3, 18]. It was shown that only a few acoustic pulses can be recorded during the linear portion of the stress-strain curve. Beyond the linear regime, acoustic emissions start to accelerate and are accompanied by macroscopic nonlinearity and stiffness decrease. Based on these observations, it is assumed that there exists a surface which separates the elastic domain from the damaging one. The material behaves elastically without damage until the thermodynamic force \mathbf{Y} reaches the damage surface g , defined as

$$g(\mathbf{Y}, \gamma) = \sqrt{\mathbf{Y} \cdot \mathbf{J} \mathbf{Y}} + \sqrt{|\mathbf{H} \cdot \mathbf{Y}|} - (\gamma + \gamma_0) \quad (10)$$

where γ_0 is a material constant representing the initial damage threshold, \mathbf{J} is a fourth-order symmetric tensor, and \mathbf{H} is a second-order symmetric tensor; their components being material parameters to be determined from experimental data. The damage characteristic tensors \mathbf{J} and \mathbf{H} are intermediate material constants that define the damage surface [34]. Determination of numerical values for these material constants from experimental data is made in the sequel by considering the various tests usually conducted to determine the strength values of a unidirectional lamina.

§3. MODELING UNIDIRECTIONAL TESTS

Since the principal directions of the damage tensor coincide with the material orientations, the characteristic tensors \mathbf{J} and \mathbf{H} are diagonal in the material (damage) principal directions (see Section 2). Therefore, they can be represented in matrix form as

$$\begin{bmatrix} J_{11} & 0 & 0 \\ 0 & J_{22} & 0 \\ 0 & 0 & J_{33} \end{bmatrix} \quad [H] = [H_1, H_2, H_3] \quad (11)$$

Then, the damage functional g is

$$g(Y, \gamma) = \sqrt{J_{11}Y_1^2 + J_{22}Y_2^2 + J_{33}Y_3^2} + \sqrt{|H_1Y_1 + H_2Y_2 + H_3Y_3|} - (\gamma + \gamma_0) \quad (12)$$

and the damage flow f is

$$f(Y, \gamma) = \sqrt{J_{11}Y_1^2 + J_{22}Y_2^2 + J_{33}Y_3^2} - (\gamma + \gamma_0) \quad (13)$$

In the absence of friction, the damage-flow function f is convex [2], and the damage characteristic tensor needs to be positive definite, or $J_{ii} > 0$. The components of the damage characteristic tensors are determined in the following sections for a single fiber-reinforced lamina by substitution of Eqs. (9) into Eq. (12).

Longitudinal uniaxial load

Let us consider a composite lamina subject to uniaxial load in the fiber direction. The only stress component different from zero is σ_1 . Then, Eq. (12) becomes

$$g = \sqrt{J_{11} \frac{\bar{C}_{11}}{\Omega_1^6} \sigma_1^2} + \sqrt{|H_1| \frac{\bar{C}_{11}}{\Omega_1^6} \sigma_1} - (\gamma + \gamma_0) \quad (14)$$

The previous equation has to be satisfied from the onset of damage up to final failure of the material. Thus, if F_{1t} and F_{1c} denote the tensile and compressive strengths of the fiber-reinforced lamina in the fiber direction, the following relations can be written:

$$\begin{aligned} \sqrt{J_{11} \frac{\bar{C}_{11}}{\Omega_{1t}^6} F_{1t}^2} + \sqrt{|H_1| \frac{\bar{C}_{11}}{\Omega_{1t}^6} F_{1t}} &= (\gamma^* + \gamma_0) \\ \sqrt{J_{11} \frac{\bar{C}_{11}}{\Omega_{1c}^6} F_{1c}^2} + \sqrt{|H_1| \frac{\bar{C}_{11}}{\Omega_{1c}^6} F_{1c}} &= (\gamma^* + \gamma_0) \end{aligned} \quad (15)$$

The parameters Ω_{1t} and Ω_{1c} are the critical values of the integrity component Ω_1 for longitudinal tensile and compressive loading conditions, respectively. In Eqs. (15), the term γ^* is representative of the value of γ at failure. At failure, the components of the integrity (damage) tensor reach their critical values, and the damage surface represented by Eq. (12) is forced to match the Tsai-Wu failure criterion. In this way, ultimate failure of a lamina is as accurate as in the Tsai-Wu criterion. Furthermore, different behavior in tension and compression as well as stress interaction is taken into account, though for the damage case the interaction takes place in the thermodynamic force space Y [Eq. (9)]. Then, the right-hand side of Eqs. (15) can be compared with the right-hand side of the analogous equations written for the Tsai-Wu failure criterion,

$$\begin{aligned} f_1 F_{1t} + f_{11} F_{1t}^2 &= 1 \\ f_1 F_{1c} + f_{11} F_{1c}^2 &= 1 \end{aligned} \quad (16)$$

indicating that in Eq. (15) at failure we have

$$\gamma^* + \gamma_0 = 1 \quad (17)$$

Therefore, Eqs. (15) can be solved for the components J_{11} and H_1 . They will turn out to be functions of the failure strength F_{1t} , F_{1c} and of the critical values of the integrity Ω_{1t} , Ω_{1c} to be determined as follows.

The magnitudes of damage at failure D_i^{cr} are estimated from statistical models of the failure process for each type of loading. If a lamina is subject to tensile stress in the fiber direction, it is reasonable to assume that the matrix carries only a small portion of the applied load and no damage is expected in the matrix during loading. The ultimate tensile strength of the composite lamina can then be accurately predicted by computing the strength of a bundle of fibers. All the fibers are assumed to remain elastic up to failure and to have the same stiffness. If a Weibull distribution is assumed for the strength of the fibers [19] and no significant initial fiber damage is assumed, the critical damage D_{1t} for longitudinal tensile loading can be computed as the area fraction of broken fibers in the lamina [20], which turns out to be a function of the Weibull shape modulus m as

$$D_{1t} = 1 - \exp\left(\frac{-1}{m}\right) \quad (18)$$

When a fiber-reinforced lamina is compressed, the predominant damage mode appears to be fiber microbuckling [21–23]. However, the buckling load of the fibers is lower than that of the perfect system because of fiber misalignment, so much that a small amount of fiber misalignment could cause a large reduction in the buckling load. For each misalignment angle α , the composite area fraction with buckled fibers $D(\alpha)$, corresponding to fibers with misalignment angle greater than α , can be taken as a measure of damage. If the fibers are assumed to have no postbuckling strength, then the applied stress is redistributed onto the remaining unbuckled fibers, which will be carrying a higher effective stress. The applied stress, which is lower than the effective stress by the factor $(1-D)$, has a maximum, which corresponds to the compressive strength of the composite. Therefore, it is possible to compute the critical damage D_{1c} for longitudinal compressive loading as

$$D_{1c} = 1 - \operatorname{erf}\left(\frac{\alpha_{cr}}{\Lambda\sqrt{2}}\right) \quad (19)$$

where erf is the error function, Λ is the standard deviation of the actual Gaussian distribution of fiber misalignment, and α_{cr} is the critical misalignment angle at failure (Eq. 23 in [21]). The value of Λ can be obtained experimentally [23] or computed using Eqs. (4.74–4.75) in [1].

Transverse uniaxial load

Let the fiber-reinforced lamina be subjected to a transverse uniaxial load, so that the only stress component different from zero is σ_2 . The expression of the damage surface (12) can be written in terms of the tensile failure strength of the material in the transverse direction,

$$\sqrt{J_{22}} \frac{\bar{C}_{22}}{\Omega_{2t}^6} F_{2t}^2 + \sqrt{|H_2|} \frac{\bar{C}_{22}}{\Omega_{2t}^6} F_{2t} = (\gamma^* + \gamma_0) = 1 \quad (20)$$

where the parameter Ω_{2t} is the critical value of the integrity component Ω_2 for tensile loading in the transverse direction. Again, the right-hand side of Eq. (20) is set to one by analogy with the Tsai-Wu criterion at failure. Using Eq. (20), the component J_{22} can be derived as a function of H_2 as

$$J_{22} = \left(1 - \sqrt{|H_2|} \frac{\bar{C}_{22}}{\Omega_{2t}^6} F_{2t} \right)^2 \left(\frac{\bar{C}_{22}}{\Omega_{2t}^6} F_{2t} \right)^{-2} \quad (21)$$

In order to determine the limiting value of the component Ω_2 of the integrity tensor, transverse tension is assumed to be controlled by brittle fracture of the matrix. As for the case of longitudinal tension, the brittle loose bundle model is assumed. The material is envisioned as a large number of matrix links surrounding the fibers. All the links remain linearly elastic until rupture and have the same stiffness but random stress values. A simple flat distribution can be assumed for the probability of matrix link failure $p(f) = 1/\sigma_o$, in terms of the strength of the strongest matrix link σ_o . Again, the area fraction of broken links represents the degree of damage of the lamina and the relevant effective stress can be computed. The applied stress has a maximum, which corresponds to the transverse tensile strength of the fiber-reinforced lamina. As can be easily derived, the maximum stress in the bundle of matrix links turns out to be $\sigma_c = \sigma_o/4$, so that the percentage of links which are broken prior to failure is [24]

$$D_{2t} = 0.5 \quad (22)$$

In-plane shear load

Let us consider the fiber-reinforced lamina subject to a state of in-plane shear, so that the only stress component different from zero is σ_6 . In this case Eq. (12), in terms of the inplane shear strength of the lamina F_6 , reduces to

$$\sqrt{\frac{J_{11}}{\Omega_{1s}^4} + \frac{J_{22}}{\Omega_{2s}^4} \frac{2\bar{C}_{66}}{\Omega_{1s}^2 \Omega_{2s}^2}} F_6^2 + \sqrt{\left| \frac{H_1}{\Omega_{1s}^2} + \frac{H_2}{\Omega_{2s}^2} \right| \frac{2\bar{C}_{66}}{\Omega_{1s}^2 \Omega_{2s}^2}} F_6 = (\gamma^* + \gamma_0) = 1 \quad (23)$$

where Ω_{1s} and Ω_{2s} are the critical values of the integrity component Ω_1 , Ω_2 for a state of in-plane shear stress. Since the shear response of a fiber-reinforced lamina along material

principal directions is independent of the sign of the shear stress, the coefficient of the linear term in Eq. (23) must be zero, leading to the relationship

$$H_2 = -\frac{\Omega_{2s}^2}{\Omega_{1s}^2} H_1 = -r_s H_1 \quad r_s = \frac{\Omega_{2s}^2}{\Omega_{1s}^2} \quad (24)$$

Then, the component H_2 can be written as a function of the parameter r_s , and the same can be done for the component J_{22} by means of Eq. (21). Hence, Eq. (23) becomes

$$\sqrt{\frac{J_{11}r_s}{k_s} + \frac{J_{22}}{k_s r_s} \frac{2\bar{C}_{66}}{k_s} F_6^2} = (\gamma + \gamma_0) = 1 \quad k_s = \Omega_{1s}^2 \Omega_{2s}^2 \quad (25)$$

Finally, with J_{11} and H_1 known from (15) and J_{22} a function of r_s from (21) and (24), Eq. (25) can be solved to obtain the value of the parameter r_s , which is then used to compute J_{22} and H_2 .

Experimental evidence reveals a highly nonlinear behavior for a fiber-reinforced lamina subject to in-plane shear. The damaged shear modulus at failure can be approximated as

$$G_{12}^* \simeq \frac{F_6}{\gamma_u} \quad (26)$$

in terms of the shear strength and the ultimate engineering shear strain of the lamina, both of which can be experimentally determined. The shear stress-strain law can be written as $\bar{\sigma}_6 = \bar{G}_{12} \bar{\gamma}_6$, where the overbar indicates effective values. An effective value of shear stiffness \bar{G}_{12} corresponds to the virgin undamaged value. Using Eq. (7) we have

$$\bar{\sigma}_6 = 2\bar{G}_{12} \Omega_1 \Omega_2 \varepsilon_6 = \frac{2G_{12} \varepsilon_6}{\Omega_1 \Omega_2} \quad (27)$$

so that at failure

$$k_s = \Omega_{1s}^2 \Omega_{2s}^2 \simeq G_{12}^* / \bar{G}_{12} \quad (28)$$

Thus, only the critical value of the product of the integrity parameters in shear can be determined, and not their individual values. This is a consequence of the assumption that the principal directions of the second-order damage tensor D remain aligned with the material principal directions over the entire life of the material. Under these conditions, shear damage is interpreted as a combination of longitudinal and transverse matrix cracks, which is supported by experimental observations [4, 25]. However, as experimentally observed, most of the damage is in the form of longitudinal cracks, so that $D_{2s} > D_{1s}$ and from Eq. (24) we obtain a restriction on the value of r_s :

$$0 < r_s < 1 \quad (29)$$

Such restriction is useful while searching for the root r_s of Eq. (25). For some material systems it is necessary to increase the values of k_s estimated with Eq. (28) in order to satisfy Eq. (29). This may be related to a higher value of damaged shear modulus than that predicted by Eq. (26), possibly due to residual deformations upon unloading.

Damage threshold and evolution law

The damage surface g and damage-flow surface f in Eqs. (12) and (13) expand as a function of the evolution variable γ . This is necessary to model the observed behavior of the material for which additional strain must be present in order for the damage to grow [26]. Lacking any experimental observation that would justify anisotropic and/or kinematic evolution, and for the sake of simplicity, we propose to use the following isotropic evolution model:

$$\gamma = -\frac{\partial \pi}{\partial \delta} = c_1 \exp\left(\frac{\delta}{c_2}\right) \quad (30)$$

where $\delta > 0$ is the evolution parameter. This evolution rule is simple enough to allow us to obtain all the coefficients (c_1, c_2) from available experimental data. Since the damage evolution portion $\pi(\delta)$ of the Helmholtz free energy must be convex in the kinematic variable δ , its second derivative has to be positive, leading to a restriction on the possible values of c_1, c_2 , as follows:

$$\pi''(\delta) = -\frac{c_1}{c_2} \exp\left(\frac{\delta}{c_2}\right) > 0 \quad (31)$$

which implies that c_1 and c_2 must have different signs. Therefore, there are two evolution equations in Eq. (30), depending on the sign of c_1 .

The actual values of the evolution parameters are derived by comparison with experimental data. Since it has been experimentally observed that the nonlinearity of the behavior of fiber-reinforced (PMC) laminae is particularly severe in the case of in-plane shear response, damage phenomena can be assumed to be very noticeable in this case. The basic idea is to adjust the evolution parameters to predict the response of a fiber-reinforced laminae subject to in-plane shear stress by means of the proposed constitutive model. Therefore, the constitutive model was compared with experimental data for in-plane shear loading (Figure 1).

The parameters γ_0, c_1 , and c_2 are determined by fitting the experimental shear stress-strain plot. When this plot is not available, but only the in-plane shear modulus G_{12} and in-plane shear strength F_6 are known, the curve can be reconstructed using

$$\sigma_6 = F_6 \tanh\left(\frac{G_{12}}{F_6} 2\varepsilon_6\right) \quad (32)$$

which is known to represent shear experimental data very well [1, 21, 25, 27–29]. Since experimental values of F_6 and G_{12} are available in the literature, all the parameters of the proposed damage evolution model can be completely identified from available data.

§4. SUMMARY

The procedure used to adjust the model parameters is summarized in this section. The damage evolution parameters c_1, c_2 control the damage evolution by Eq. (30). The damage threshold γ_0 represents the initial size of the damage surface, Eq. (12). No damage can occur until the thermodynamic forces \mathbf{Y} reach the damage surface. These three parameters are adjusted with the shear stress-strain diagram for monotonic loading (e.g., Figure 1).

The internal material constants $J_{11}, J_{22}, H_1, H_2, r_s$, and k_s are used to write the model equations in a concise form. These are not adjustable model parameters since their values

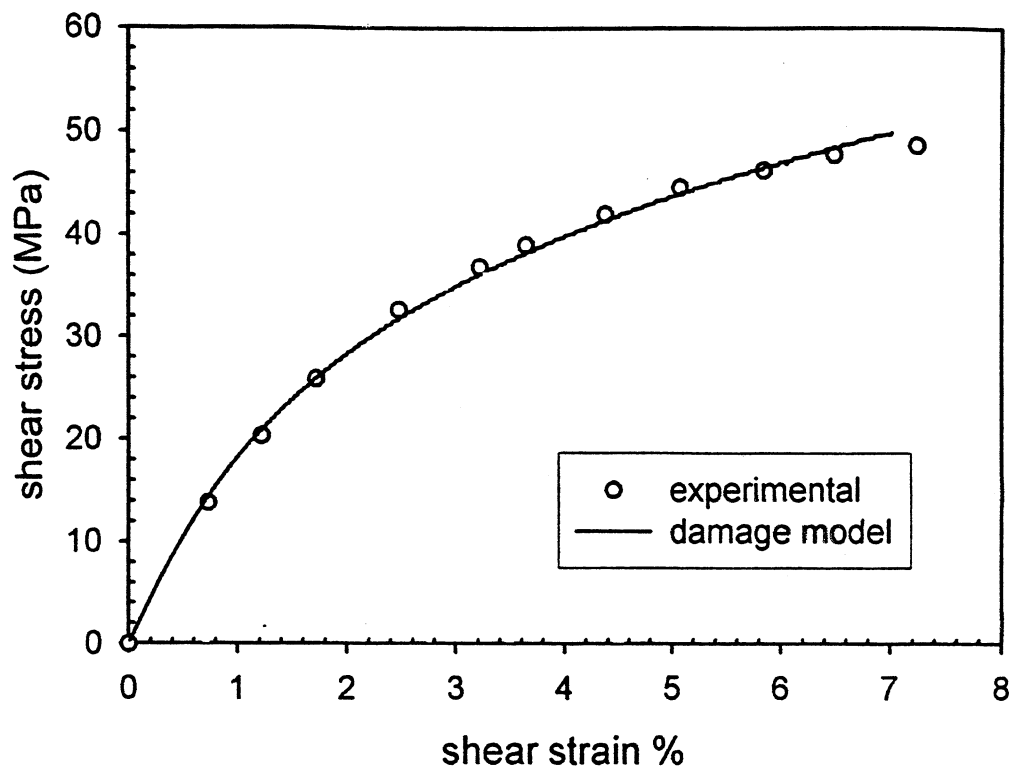


Figure 1. Experimental and model results for shear test of aramid/epoxy unidirectional lamina.

are univocally determined in terms of the available material constants F_{1t} , F_{1c} , F_{2t} , F_{2c} , F_6 , γ_u , and the critical damage values D_{1t} , D_{1c} , D_{2t} . The later are fixed values in terms of material constants m and Λ as described by Eqs. (18), (19), and (22). The Weibull dispersion of fiber strength m and the misalignment angle Λ are available from the literature [28–31] and well-established procedures exit to measure them for new materials [23, 32]. Finally, the material constants E_1 , E_2 , G_{12} , and ν_{12} are readily available. The only information that is not readily available is the shear stress–strain plot (e.g., Figure 1), which is necessary to adjust the damage evolution parameters (c_1 , c_2 , γ_0). The plot can be approximated in terms of G_{12} and F_6 by Eq. (32), or it can be determined experimentally using a shear test fixture such as described in ASTM D5379 [12].

§5. MODEL VALIDATION

In this section we use available experimental data for unidirectional laminae to find all the parameters in the damage constitutive equations. Then, we use laminate data to validate the predictions of the model.

Aramid/epoxy

The experimental data of [13–15] for unidirectional aramid/epoxy is reproduced in Table 1 and used in this section to fit the model parameters. First the critical damage values in tension, compression, and shear were obtained according to Eqs. (18), (19), and (28), assuming a Weibull shape modulus $m = 9$. Then, Eqs. (15), (21), and (25), are solved for r_s , J_{11} , J_{22} , H_1 , H_2 [subject to condition Eq. (29)]. Next, the model is solved incrementally with an applied in-plane shear strain to adjust the parameters γ_0 , c_1 , and c_2 , using the shear

Table 1
Available experimental data

Property	Aramid-Epoxy	T300-914	T300-5208
E_1 [Pa]	7.34E + 10	1.42E + 11	1.36E + 11
E_2 [Pa]	5.50E + 09	10.3E + 09	9.80E + 09
G_{12} [Pa]	2.30E + 09	7.20E + 09	5.20E + 09
ν_{12}	0.27	0.27	0.28
F_{1r} [pa]	1.14E6	1.83E + 09	1.55E + 09
F_{1c} [Pa]	2.13E + 08	1.09E + 09	1.09E9
F_{2r} [Pa]	2.74E + 07	5.70E + 07	5.90E + 07
F_6 [Pa]	4.74E + 07	8.60E + 07	7.50E + 07

stress-strain experimental data, as shown in Figure 1. The resulting model parameters are reported in Table 2.

Then, with fixed values for all the parameters, the model is used to predict the behavior of available experimental data from off-axis tests for the same material, as shown in Figure 2.

T300/5208 and T300/914 carbon/epoxy

The analysis of available experimental data for T300/5208 [13] and T300/914 [16] allows us to demonstrate the accuracy of the model for predicting the behavior of laminates.

Using experimental data presented in Table 1, and assuming the Weibull parameter $m = 9$, it is possible to derive the critical damage values D_{1c} , D_{1r} , D_{2r} using Eqs. (18), (19), and (28). The components of the **J** and **H** tensors are determined solving the system given by Eqs. (15), (21), and (25). Finally, the evolution parameters c_1 , c_2 , γ_0 are adjusted in such a way that the model results match well the shear experimental curve. Since the actual experimental plot is not available, it was reconstructed from available experimental data of F_6 and G_{12} using Eq. (32). A comparison between the model results and the reconstructed

Table 2
Model parameters determined with available data from Table 1

Property	Aramid-Epoxy	T300-914	T300-5208
k_s	0.865	0.5972	0.631
D_{1r}^{cr}	0.125161	0.1161	0.1161
D_{1c}^{cr}	0.110945	0.110945	0.110945
D_{2r}^{cr}	0.5	0.5	0.5
J_{11}	4.65E-14	2.52E-14	1.56E-15
J_{22}	1.38E-13	1.16E-12	1.23E-13
H_1	7.52E-07	0.1297E-7	3.00E-12
H_2	-3.25E-07	-0.755E-8	-1.27E-12
r_s	0.706760603	0.580899	0.421789122
γ_0	0	-0.17	0
C_1	0.04	0.17	0.02
C_2	-5.00E + 04	-8.9E + 05	-1.00E + 06

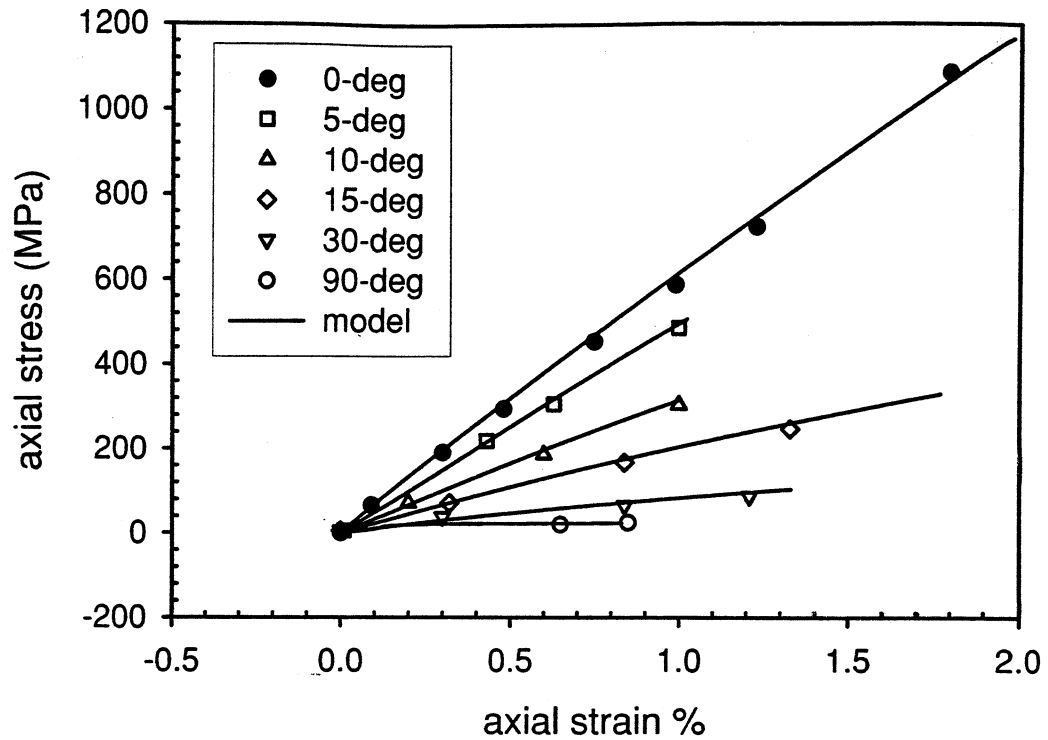


Figure 2. Experimental and model results for off-axis test of aramid/epoxy unidirectional lamina.

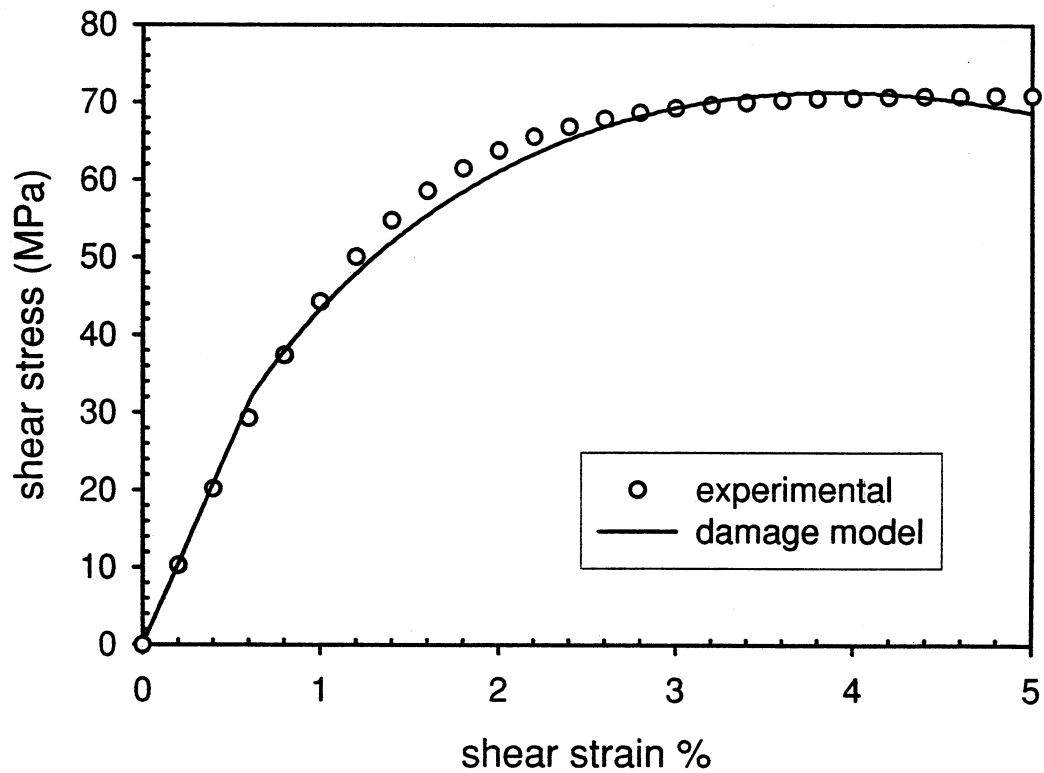


Figure 3. Experimental and model results for shear test of T300/5208 unidirectional lamina.

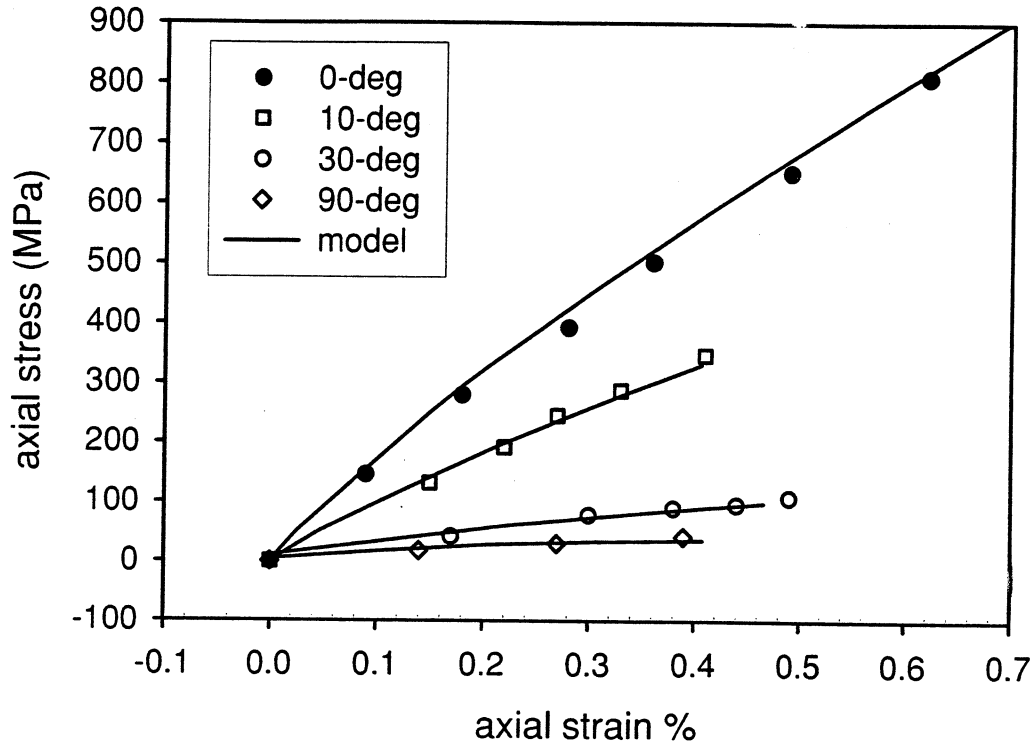


Figure 4. Experimental and model results for off-axis test of T300/5208 unidirectional lamina.

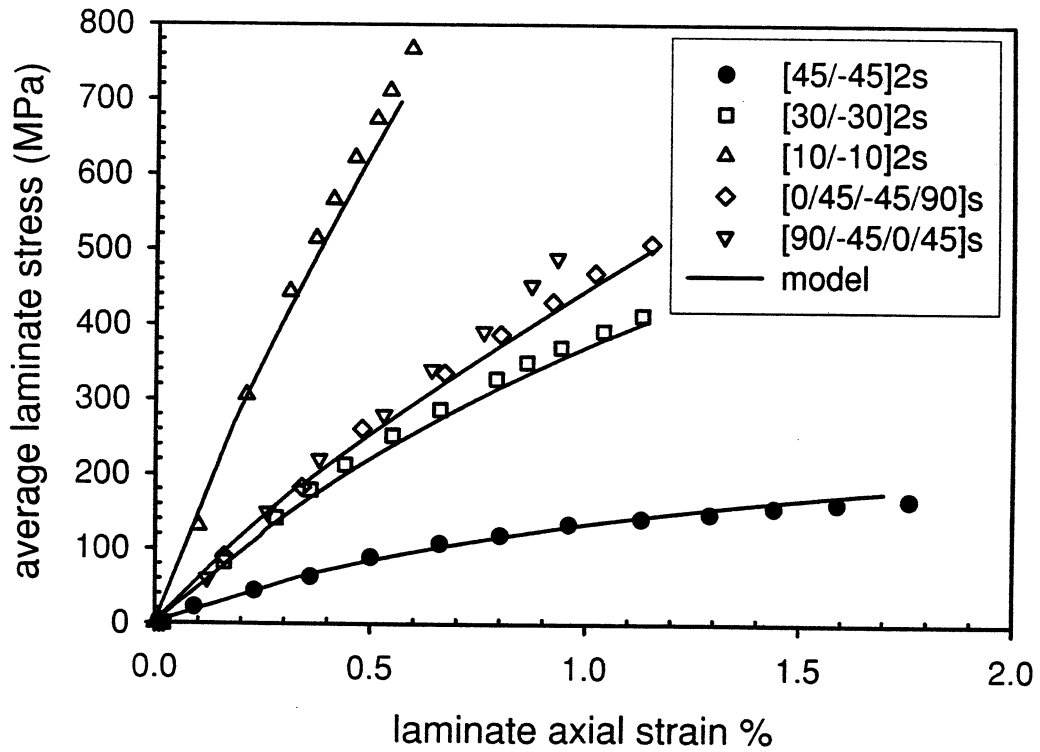


Figure 5. Experimental and model results for tensile test of T300/5208 laminate.

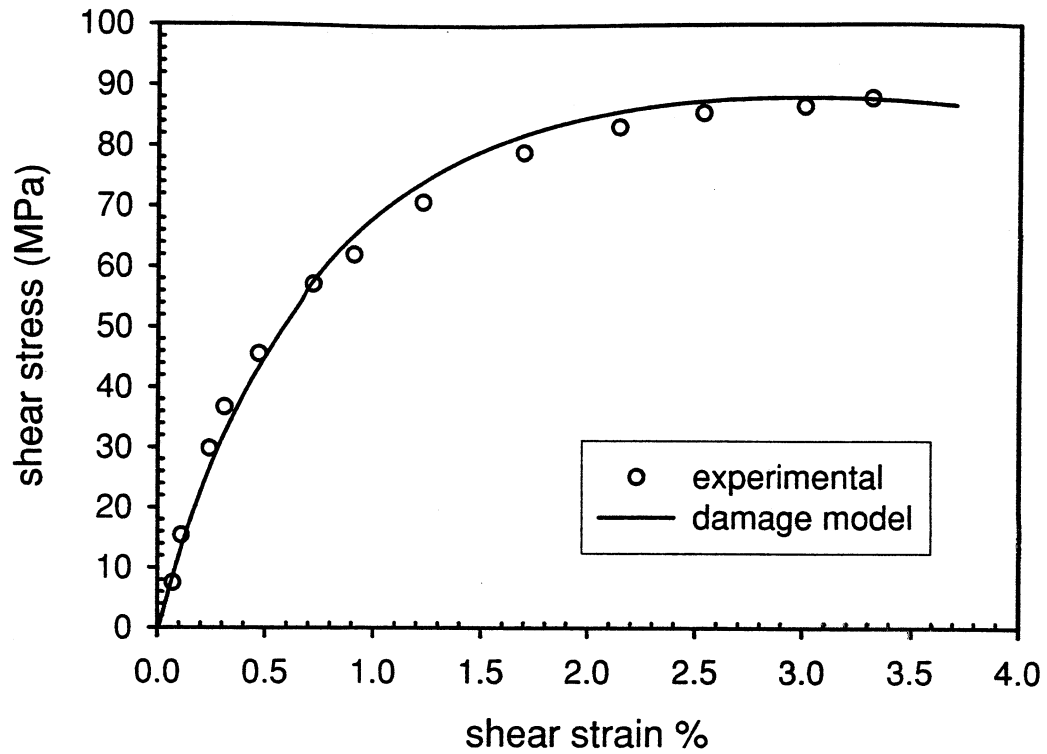


Figure 6. Experimental and model results for shear test of T300/914 unidirectional lamina.

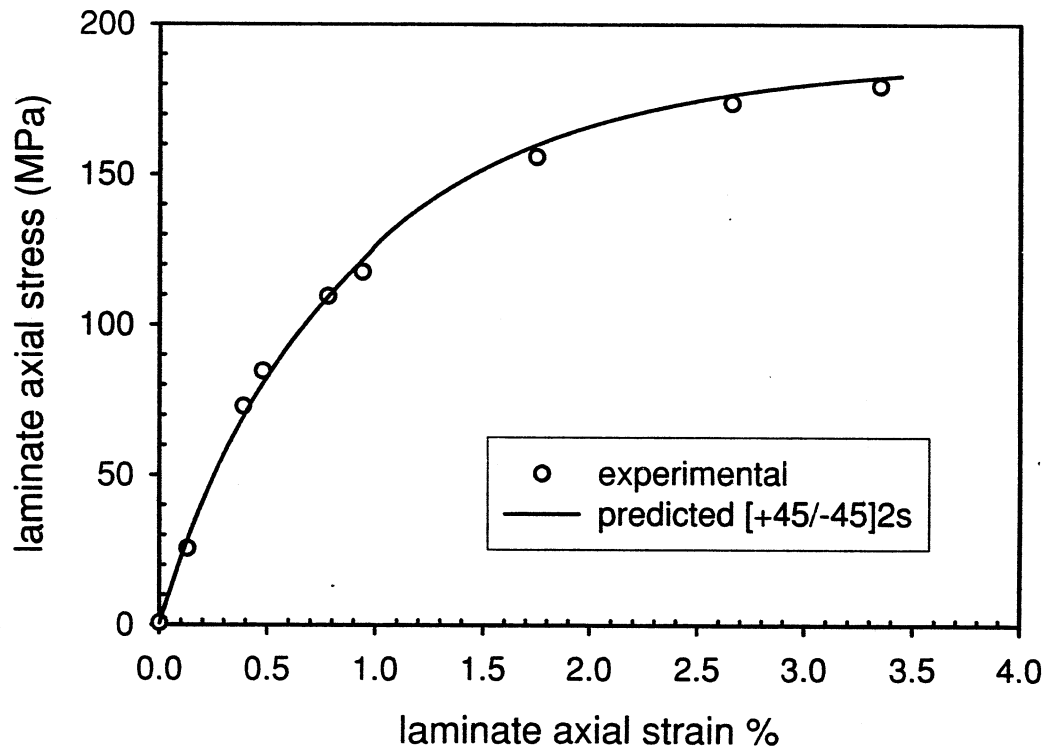


Figure 7. Experimental and model results for tensile test of T300/914 laminate.

experimental data is shown in Figure 3 for T300/5208 and in Figure 6 for T300/914. It is worth noting that the failure condition is reached when the predicted damage values D_i match the critical values D_{ic} .

Next, keeping all the parameters unchanged, the behavior of several off-axis tests are predicted and compared to experimental data in Figure 4. The damage model is used to predict the behavior of various laminates, as shown in Figure 5, for T300/5208. It can be observed that the predictions are quite good. Furthermore, the predicted and observed behavior of $[+/-45]_{4s}$ laminates made of T300/914 is shown in Figure 7.

§6. CONCLUSIONS

The main advantage of the model proposed is its simplicity. All the parameters in the model can be evaluated from lamina experimental properties that are usually available or that can be easily determined by standardized experimental procedures. The model proposed has the ability to account for different damage behavior and ultimate strength in tension and compression along the fiber direction of individual laminae within a laminate. Furthermore, the model accurately represents the shear stress-strain plot, yielding the observed behavior with regard to the resulting damage accumulation during the shear test. It is this latter feature that accounts for the success of the model when predicting the off-axis tests of a lamina. The damage within each lamina of a laminate and consequent stress redistribution among laminae is accounted for by the model. The model appears to predict correctly the stiffness reduction due to damage. The ultimate strength is also predicted, which is to be expected since the damage surface reduces to the Tsai-Wu failure criterion when the internal damage measures reach the critical values.

Friction at the fiber-matrix interphase and/or between plies would render the system nonconvex, with consequent increase of difficulty in the formulation. The three-dimensional stress field produced by matrix cracks in 90° plies and other characteristic damage states may need a more refined analysis. Similarly, the model proposed cannot reveal microscopic features such as periodicity of cracks and so on. On the other hand, the attractive feature of the proposed model is that standard test data can be employed for the determination of the damage parameters. Although the derivation of the model is complex, its utilization is not. Thus it has the potential to be a useful tool for the practicing engineer in predicting, in an average sense, the inelastic response of composite laminates due to damage accumulation.

REFERENCES

- [1] E. J. Barbero, *Introduction to Composite Materials Design*, Taylor & Francis, New York, 1999.
- [2] J. Lemaitre and J.-L. Chaboche, *Mechanics of Solid Materials*, Cambridge University Press, Cambridge, UK, 1990.
- [3] A. Mittelman and I. Roman, Tensile Properties of Real Unidirectional Kevlar/Epoxy Composites, *Composites*, vol. 21, no. 1, pp. 63-69, 1990.
- [4] M. R. Piggott, K. Liu, and J. Wang, New Experiments Suggest that All the Shear and Some Tensile Failure Processes Are Inappropriate Subjects for ASTM Standards, *ASTM STP 1383, Composite Structures: Theory and Practice*, ASTM, Philadelphia, 2000.
- [5] A. Razvan, C. E. Bakis, and K. L. Reifsnider, SEM Investigation of Fiber Fracture in Composite Laminates, *Mater. Charact.*, vol. 24, no. 2, pp. 179-190, 1990.
- [6] S. A. Salpekar, and T. K. O'Brien, Analysis of Matrix Cracking and Local Delamination in $(0/\theta/-\theta)_s$ Graphite Epoxy Laminates under Tensile Load, *J. Composites Technol. Res.*, vol. 15, no. 2, pp. 95-100, 1993.

- [7] T. K. O'Brien, Stacking Sequence Effect on Local Delamination Onset in Fatigue, *Proc. Int. Conf. on Advanced Composite Materials*, pp. 399–406, Minerals, Metals & Materials Society (TMS), Warrendale, PA, 1993.
- [8] Y. Kim, J. F. Davalos, and E. J. Barbero, Progressive Failure Analysis of Laminated Composite Beams, *J. Composite Mater.*, vol. 30, no. 5, pp. 536–560, 1996.
- [9] G. Z. Voyiadjis and T. Park, Anisotropic Damage of Fiber-Reinforced MMC Using Overall Damage Analysis, *J. Eng. Mech.*, vol. 121, no. 11, pp. 1209–1217, 1995.
- [10] G. Z. Voyiadjis and T. Park, Local and Interfacial Damage Analysis of Metal Matrix Composites, *Int. J. Eng. Sci.*, vol. 33, no. 11, pp. 1595–1621, 1995.
- [11] G. Z. Voyiadjis and A. R. Venson, Experimental Damage Investigation of a SiC-Ti Aluminide Metal Matrix Composite, *Int. J. Solids Struct.*, vol. 4, pp. 338–361, 1995.
- [12] *American Society for Testing Materials*, vol. 15.8, ASTM, Philadelphia, 2000.
- [13] C. T. Herakovich, *Mechanics of Fibrous Composites*, Wiley, New York, 1998.
- [14] M. J. Pindera, Z. Gurdal, J. S. Hiddle, and C. T. Herakovich, Mechanical and Thermal Characterization of Unidirectional Aramid/Epoxy, CCMS8629, Center for Composite Materials and Structures, Virginia Tech., Blacksburg, VA, 1987.
- [15] M. J. Pindera, Shear Testing of Fiber Reinforced Metal Matrix Composites, in *Metal Matrix Composites: Testing Analysis, and Failure Modes*, ASTM STP 1032, p. 1945, W. S. Johnson (ed.), American Society for Testing and Materials, Philadelphia, 1989.
- [16] P. Ladeveze and E. LeDantec, Damage Modelling of the Elementary Ply for Laminated Composites, *Composites Sci. Technol.*, vol. 43, pp. 257–267, 1992.
- [17] S. Nemat-Nasser and M. Hori, *Micromechanics: Overall Properties of Heterogeneous Materials*, North-Holland, Amsterdam, 1999.
- [18] Y. M. Liu, T. E. Mitchell, and N. G. Wadley, Anisotropic Damage Evolution in Unidirectional Fiber Reinforced Ceramics, *Acta Mater.*, vol. 45, no. 10, pp. 3981–3992, 1997.
- [19] B. W. Rosen, The Tensile Failure of Fibrous Composites, *AIAA J.*, vol. 2, no. 11, pp. 1985–1911, 1964.
- [20] K. Kelly and E. J. Barbero, The Effect of Fiber Damage on the Longitudinal Creep of a CFMMC, *Int. J. Solids Struct.*, vol. 30, no. 24, pp. 3417–3429, 1993.
- [21] E. J. Barbero, Prediction of Compression Strength of Unidirectional Polymer Matrix Composites, *J. Composite Mater.*, vol. 32, no. 5, pp. 483–502, 1998.
- [22] W. L. Yin, A New Theory of Kink Band Formation, AIAA-92-2552-CP, 1992.
- [23] S. W. Yurgartis and S. S. Sternstein, Experiments to Reveal the Role of Matrix Properties and Composite Microstructure in Longitudinal Compression Response of Composite Structures, ASTM, Nov. 16–17, 1992.
- [24] J. Janson and J. Hult, Damage Mechanics and Fracture Mechanics: A Combined Approach, *J. Mech. Appl.*, vol. 1, pp. 69–84, 1977.
- [25] E. J. Barbero and E. A. Wen, Compressive Strength Prediction for Production Parts without Compression Testing, *ASTM STP-1383, Composite Structures: Theory and Practice*, ASTM, Philadelphia, 2000.
- [26] G. Z. Voyiadjis and B. Deliktas, A Coupled Anisotropic Damage Model for the Inelastic Response of Composite Materials, *Comput. Meth. Appl. Mech. Eng.*, vol. 183, pp. 159–199, 2000.
- [27] E. J. Barbero and J. Tomblin, A Damage Mechanics Model for Compression Strength of Composites, *Int. J. Solids Struct.*, vol. 33, no. 29, pp. 4379–4393, 1996.
- [28] J. G. Haberle, Strength and Failure Mechanisms of Unidirectional Carbon Fibre-Reinforced Plastics under Axial Compression, Ph.D. thesis, Imperial College, London, U.K. 1991.
- [29] E. Wen, Compressive Strength Prediction for Composite Unmanned Aerial Vehicles, thesis, West Virginia University, Morgantown, WV, 1999.
- [30] W. G. McDonough and R. B. Clough, The Measurement of Fiber Strength Parameters in Fragmentation Tests by Using Acoustic Emissions, *Composites Sci. Technol.*, vol. 56, pp. 119–1127, 1996.
- [31] Y. Kasai and M. Saito, Weibull Analysis of Strengths of Various Reinforcing Filaments, *Fibre Sci. Technol.*, vol. 12, pp. 21–29, 1979.

- [32] C. R. Schultheiz, W. G. McDonough, K. Shrikant, C. L. Shutte, K. S. Mcturk, M. McAulife, and D. L. Hunston, *13th Symp. on Composites Testing and Design*, pp. 257–286, ASTM, Philadelphia.
- [33] B. Liu and L. B. Lessard, Fatigue and Damage Tolerance Analysis of Composite Laminates: Stiffness Loss, Damage Modeling and Life Prediction, *Comput. Sci. Technol.*, vol. 51, pp. 43–51, 1994.
- [34] E. J. Barbero and L. DeVivo, A Constitutive Model for Elastic Damage in Fiber-Reinforced PMC Laminae, *J. Damage Mech.*, vol. 10, no. 1, pp. 73–93, 2001.